# A Mechanistic Description of Aerosol Transport and Deposition in Stress Corrosion Cracks

Stylianos Chatzidakis*, John Scaglione

*Oak Ridge National Laboratory, One Bethel Valley Road, Oak Ridge, TN 37831*
**chatzidakiss@ornl.gov*

***Abstract:*** *Under certain conditions, dry storage confinement leak tightness could yield a release of radioactive aerosols to the environment through penetrating canister cracks. While considerable progress has been made in quantifying the source term, little attention has been given to the leakage itself or to the source term–reducing processes inside the leak path. Limited experimental evidence is available on the importance of aerosol retention in chloride-induced stress corrosion cracks through stainless steel canisters. Nevertheless, the accuracy of consequence assessments can be improved by accounting for the leak path deposition of aerosol in the source term. The filtration effect of such cracks is relevant to the source term assessments. An important side effect of aerosol deposition in leak paths could be the plugging of the leak path. Further research into this phenomenon is desirable. The purpose of the present work is to introduce a generic, reliable numerical model for prediction of aerosol transport, deposition, and plugging in leak paths that are similar to stress corrosion cracks while accounting for potential plugging formation. The model is dynamic (changing leak path geometry due to plugging), and it relies on the numerical solution of the aerosol transport equation in one dimension using finite differences. An extensive validation exercise (particle diameters: 0.01–10 μm and pressure difference up to 12 kPa) was conducted based on comparisons with experimental and theoretical data. The developed model is fairly general, since it is based on a generic mechanistic description of the aerosol flow and particle deposition in the leak path. The developed model does not require experimental fittings other than using the leak rate parameters commonly available in practical applications. The approximate agreement with the experimental data demonstrates the model predictions can be qualified as representative. This is a major achievement of the model, which was based on generic aerosol mechanics with no reference to or adjustment for experimental data.*

## I. INTRODUCTION

Previous work has identified existing dose consequence evaluations, including quantifying the source term, determining release fractions, and defining the exposure conditions.[1] However, particle penetration through the confinement boundary may be significantly lower, even by orders of magnitude, in comparison to that associated with the leakage rate. Earlier work on particle transport through concrete cracks and nuclear containments has shown that under certain conditions, the penetration fraction can be significantly reduced. Mosley et al.[2] designed a chamber to measure particle penetration through horizontal slits between aluminum plates for a range of particle diameters (0.05–5 μm) and found that particle penetration is a strong function of particle size. Experiments for idealized rectangular cracks showed that particles of 0.1–10 μm have the highest penetration efficiency.[3] For horizontal fine capillaries, the significance of the three main deposition mechanisms (Brownian, gravitational, impaction) was determined by capillary radius, length, and fluid velocity.[4] More recent experiments showed that a significant quantity of particulate mass is retained within the crack volume.[5]

The purpose of this work is to explore particle penetration through leakage paths in chloride-induced stress corrosion cracking (CISCC) and to introduce and validate a numerical model of aerosol transport, deposition, and plugging through capillaries, slots, and cracks. This effort includes (i) development of a numerical model to analyze the various deposition processes in leak paths and provide quantitative estimates of penetration factors, as well as an understanding of the variables that affect them, (ii) confirmation of model validity with theoretical and experimental data, and (iii) parametric analysis for different CISCC scenarios including various particle sizes, pressures, and crack dimensions.

This report does not address aerosol leakage during depressurization (i.e., transient state); instead, it focuses on any effects following depressurization and when pressure differences are small, e.g., $\Delta P<200$ Pa. However, the

authors recognize that significant aerosol leakage may occur during depressurization, so the model will be developed and validated to facilitate transient state calculations.

## II. APPROACH

This section briefly describes the proposed phenomenological model of aerosol transport, deposition, and plugging through capillaries, slots, and cracks. The model is based on the aerosol general dynamic equation and can simulate rough or smooth surfaces, irregular geometries, and unsteady flow. Four main deposition mechanisms (gravitational, Brownian diffusion, turbulent diffusion, and eddy impaction) have been included. Laminar, transition, and turbulent gas flow regimes have also been included in the model. The proposed model was tested and compared with experimental and theoretical work to evaluate its validity and to identify its range of applicability. Overall, the model can predict important quantities such as plug mass, gas passed, plugging time, plug profile, and penetration fraction.

### II.A. General Equations

The principle of mass conservation is applied to describe aerosol transport in a container. The general mass balance requires:

$$\begin{aligned} &rate\ of\ change\ of\ aerosol\ concentration \\ &\quad = inflow - outflow \\ &\quad - deposition\ within\ container \end{aligned}$$

For example, the principle of mass conservation when applied to aerosol particles inside a stainless steel canister is:

$$\frac{dC_1}{dt} = -\frac{QC_1}{V_1} - \left(K_{1g} + K_{1d}\right)C_1, \quad (1)$$

where $C_1$ is the particle concentration, t is time, Q is the volumetric flowrate, $V_1$ is the canister's free volume, $K_{1g}$ is the particle decay rate due to gravitational settling, and $K_{1d}$ is the particle decay rate due to diffusion to the surfaces. The first term on the right side represents the rate at which particles are removed from the canister by airflow. The second term represents the rate at which particles are removed by deposition mechanisms on surfaces other than the stress corrosion crack. Outside the canister, mass balance requires the following:

$$\frac{dC_2}{dt} = \frac{PQC_1}{V_1} - \frac{QC_2}{V_2} - \left(K_{2g} + K_{2d}\right)C_2, \quad (2)$$

where $C_2$ is the particle concentration outside the canister (e.g., overpack-canister gap), P is the penetration factor (i.e., the fraction of particle concentration leaving the canister and arriving outside), $K_{2g}$ is the particle decay rate due to gravitational settling, and $K_{2d}$ is the particle's decay rate due to deposition mechanism by diffusion. The penetration factor is typically derived empirically and calculated as the product of different deposition mechanisms. For example, if gravitational and diffusion depositions are the only mechanisms, then the penetration factor is

$$P = P_g P_d, \quad (3)$$

where $P_g$ is the deposition due to gravitational diffusion and $P_d$ is the deposition due to Brownian diffusion. Empirical penetration factors have been proposed.[6, 7] Alternatively, a more flexible, accurate way to calculate the particle deposition would be to use a phenomenological model, as proposed herein.

### II.B. Gas-Flow Modeling

To describe gas flow in a leak path, a theoretical approach by Williams (1994) is used.[8] This approach is simple and effective in capturing the essential features of the flow in a narrow leak path. Assuming isothermal flow, the flow field can be derived by solving the equations of continuity and momentum, which in one-dimensional steady-state form, are as follows:[8]

Continuity:

$$\rho_g \mathrm{Au} = \mathrm{Q}_m, \quad (4)$$

Momentum:

$$\rho_g u \frac{\mathrm{du}}{\mathrm{dx}} + \frac{\mathrm{dp}}{\mathrm{dx}} + 2\rho_g C_f \frac{u^2}{D_H} = 0, \quad (5)$$

where $C_f$ is the friction factor that depends mainly on Reynolds number. The fluid density $\rho_g$ is related with the pressure p and the temperature T through the state equation $p = \rho \cdot R_g \cdot T$, where $R_g$ is the gas constant. Using these equations, the mass flow rate $Q_m$ can be written as a function of the pressure drop along the flow direction:

$$p_u^2 - p_d^2 = R_g T Q_m^2 \int_0^L C_f(\mathrm{Re}) \frac{\chi(x)}{A^3(x)} \mathrm{dx}, \quad (6)$$

where x is the axial distance from the inlet of the crack (or capillary), $p_u$ and $p_d$ are the pressure at the upstream and at the downstream of the crack, respectively, L is the length of the duct, $\chi$ is the perimeter of the duct, and A is the cross sectional area. This equation can be solved numerically to determine the mass flow rate $Q_m$. When this is known, the velocity and volume flow rate can be calculated using the mass continuity equation.

For constant cross section, Eq. (6) can be written in a simplified form:

$$Q_m^2 = \frac{A^3\left(p_u^2\text{-}\mathrm{p}_d^2\right)}{\chi C_f L \mathrm{R}_g \mathrm{T}}. \quad (7)$$

The transition from laminar to turbulent flow for pipes takes place at Re=2300. However, recent experiments with microcracks or capillaries with micrometer diameters suggest that transition can occur much earlier, at Re numbers as low as 5–10 for rectangular geometries and Re=400–600 for cylindrical geometries. This results in the need for new friction factor correlations. Derived empirical correlations for friction factor at transition from laminar to turbulent flow regime are as follows:

for crack-like geometries and Re>5:[9]

$$C_f = 0.25\left(\frac{2.11}{1+\log\left(Re^{1/2}\right)}\right)^{6.7683}, \text{ and} \quad (8)$$

for capillaries and Re>400:

$$C_f = 0.0025\left(5+\left(\frac{10^6}{Re}\right)^{1/3}\right). \quad (9)$$

### II.C. Aerosol Transport Equation

In the presence of a gas flow, the general dynamic equation (GDE) in three-dimensional space for the case of aerosol penetration through a crack is reduced to a transport equation which can be written in one-dimensional form as follows:[10]

$$\frac{\mathrm{dC(x,t)}}{\mathrm{dt}} + \frac{1}{A(\mathrm{x,t})}\frac{d}{dx}\left[A(\mathrm{x,t})\cdot u(\mathrm{x,t})\cdot C(\mathrm{x,t})\right] = -\mathrm{V}_d(\mathrm{x,t})\frac{\chi(\mathrm{x,t})}{A(\mathrm{x,t})}C(\mathrm{x,t}), \quad (10)$$

where C is the aerosol mass concentration, $V_d$ is the deposition velocity, A is the cross-sectional area, $\chi$ is the wetted perimeter of the cross section, and u is the gas velocity. All previous parameters are functions of the axial coordinate x and time t. The deposition velocity is calculated as the sum of the deposition velocities corresponding to each individual mechanism. In this paper, four deposition mechanics are considered: gravitational settling, Brownian diffusion, inertial impaction, and eddy impaction for the case of turbulent flow conditions. These deposition mechanisms are very common at the aerosol penetration investigation, and they also play a crucial role in aerosol retention.

### II.D. Deposition Mechanisms

The deposition velocities for the four main deposition mechanisms—gravitational settling, Brownian diffusion, turbulent diffusion, and eddy impaction—are described below.

*Gravitational settling:* The deposition velocity due to gravitational settling is written as follows:[10]

$$V_{d(sed)} = \tau g \sin\theta, \quad (11)$$

where:

$$\tau = \frac{\rho_p d_p^2 C_c}{18\mu_g}. \quad (12)$$

Angle θ is the angle between the airway direction and the force of gravity (the so-called *gravity angle*), $\rho_p$ is the particle's density, $d_p$ is the particle's diameter, $C_c$ is the Cunningham slip correction factor that depends on the particle's size, g is the acceleration due to gravity, and $\mu_g$ is the dynamic viscosity of the gas.

*Brownian diffusion:* The deposition velocity due to Brownian diffusion is determined using mass transfer theory. It is expressed in terms of the concentration boundary layer thickness, where according to the heat-mass transfer theory analogy, the Nusselt number is replaced by the Sherwood number Sh. Specifically,[11]

$$V_{d(diff)} = \frac{D_B Sh}{D_H}, \text{ and} \quad (13)$$

$$D_B = \frac{k_B T_g C_C}{3\pi\mu_g d_p}, \quad (14)$$

where $D_H$ is the hydraulic diameter of the crack and $D_B$ is the diffusion coefficient. The Sherwood number is specified as a function of distance from the beginning of the crack to properly account for entrance effects. The algebraic fittings used provide the local Sherwood number as a function of the dimensionless length $x^+$, as follows:[12]

$$x^+ = \frac{x}{D_H \mathrm{ReSc}_p}, \quad (15)$$

$$\mathrm{Sh}(x^+) = \begin{cases} 1.077(x^+)^{\frac{-1}{3}}\text{-}0.7, & x^+ \le 0.01 \\ 3.657+6.874\left(10^3 x^+\right)^{-0.488}\exp(-57.2x^+), & x^+ > 0.01 \end{cases}. \quad (16)$$

*Inertial impaction:* The deposition velocity due to inertial impaction is written as follows:

$$V_{d(inert-imp)} = uStkD_H\pi/L_c, \quad (17)$$

where $u$ is the gas velocity and $L_c$ the length of the curved branching zone.

*Turbulent diffusion:* In case of turbulent flow, the mechanism of eddy diffusion is considered. Molecular (Brownian) diffusion can be neglected in this case. The deposition velocity due to eddy diffusion is determined by using the standard correlation given below:[13]

$$V_{d(turb-diff)} = 0.2 u_{fr} Sc_p^{-2/3} Re^{-1/8}, \tau^+ < 0.3, \quad (18)$$

where $u_{fr}$ is the friction velocity.

*Eddy impaction:* Eddy impaction comes into effect only when the flow is turbulent. In a turbulent fluid, there is an ensemble of eddies of varying size and intensity. Depending on their size and mass, particles tend to become entrained within the eddies and follow the eddies' motion. Eddy impaction velocity will be written in terms of friction velocity $u_{fr}$ and reduced stopping time $\tau^+$, as follows:[10]

$$V_{d(\text{turb})} = min\left[6\times10^{-4}(\tau^+)^2 u_{fr}, 0{,}1 u_{fr}\right], \tau^+ > 0.3. \quad (19)$$

*Total deposition velocity:* The total deposition velocity is given as the algebraic sum of the deposition velocities corresponding to each individual mechanism described previously, namely:

$$V_d = \begin{cases} V_{d(sed)} + V_{d(diff)} + V_{d(inert-imp)} & (laminar), \\ V_{d(sed)} + V_{d(diff)} + V_{d(inert-imp)} & (turbulent). \end{cases} \quad (20)$$

The implicit assumption permitting the algebraic addition of the individual velocities is that the deposition mechanisms are independent of each other.

### II.E. Plugging

A leak path through which aerosol passes may become plugged. The particulate matter will deposit on the surface, changing the internal geometry of the flow area. Eventually the plug's mass will increase, leading to a complete obstruction of the pathway. There is experimental evidence that other possibilities exist, such as rebound of particles or plug fragmentation at some stage in the deposition progress.[14] The present analysis is limited to addressing the case of a continuous build-up of deposits until the path is completely plugged. The mass of the deposit up to any position S can be obtained in terms of the deposition velocity and the particle concentration, as follows:[15]

$$M_{dep} = \int_0^S \int_0^t 2\pi R C V_d \, dx \, dt. \quad (21)$$

Assuming that the deposit material is homogeneous with a density equal to the density of the particles, then the volume of the deposit can be directly derived from its mass:

$$V_{dep} = \frac{M_{dep}}{\rho_p}. \quad (22)$$

In Eq. (22) above, density $\rho_p$ is assumed to be the bulk material density. This approximation is more accurate for large particles that are deposited mainly by gravity or eddy impaction. The deposition of particles is assumed to occur uniformly on the path's circumference. This assumption is valid for mechanisms such as diffusion (Brownian or turbulent) or eddy impaction, but it is approximate for directional mechanisms such as gravitational settling. Under this assumption, the change in radius due to plugging is related to the deposit volume, as follows:

$$dR = \frac{1}{2\pi R} \frac{dV_{dep}}{dx}. \quad (23)$$

### II.F. Numerical Solver

The numerical solution first calculates the fluid velocity in each time step. Then the particle transport equation is solved using an implicit finite difference scheme. The upwind scheme is used for the discretization of the convection term, which is the second term on the left-hand side of Eq. (10). The duct radius is then updated according to Eq. (23) through calculating the amount of the deposited mass, as shown in Eqs. (21) and (22). All the numerical integrations required in this calculation are performed using the trapezoidal rule. The new cross section is then used for the aerosol calculations in the next step.

## III. BENCHMARKING

To illustrate and evaluate the proposed aerosol transport model, the model was benchmarked against real experimental cases of particle penetration and plugging in leak paths under a variety of conditions in tubes or real cracks. The experiments are focused on penetration of particles through the cracks of a naturally broken brick (Liu and Nazaroff, 2003) and on penetration of particles through a cracked reinforced concrete sample (by Gelain and Vendel, 2007).

### III.A. Comparison with Experiments by Gelain and Vendel (2007)

The experiments performed by Gelain and Vendel (2007) concern the penetration of a particle through a real crack network that was created in a reinforced concrete slab measuring 128 cm × 75 cm × 10 cm. The sample wall was cracked by subjecting it to shear stresses from alternate directions. The tests were performed with monodisperse aerosols with particles between 50 nm and 4 μm. The aerosol penetration fraction was measured as a function of the imposed pressure difference across the concrete slab as a function of the flowrate leaking through the crack network. With the coarse particles of 4 μm, the aerosol was completely trapped in the cracks. The results for the 1 μm aerosol diameter have shown a partial retention. Fig. 1 shows the penetration fraction of particles as calculated

with the model developed for this effort and compares the calculated results with the measured data. The following observations are made:

- The present model gives satisfactory results when compared with the experimental measurements of Gelain and Vendel, and it is also in close agreement with their model. Generally, both models display similar performances.
- The present model gives a more consistent prediction for low flow rates. While Gelain's model (2007) predicts values higher than 1.0, the model developed for the current effort predicts that the penetration fraction will asymptotically reach 1.0, a behavior more consistent with the measured data.
- All particles having diameters of $d_p$=4.1 μm are retained, with no penetration, within the channel, independent of flow rate.
- Particles of several microns can hardly penetrate through cracks because of the highly efficient removal of such particles by interaction deposition or gravitational settling.

### III.B. Comparison with Experiments by Liu and Nazaroff (2003)

Liu and Nazaroff (2003) experimentally studied the penetration of particles through cracks of typical building materials. They used cracks of well-defined, controlled geometry by machining the material samples, but they also created real cracks by breaking a brick. Results from the latter tests were selected in the present work to imitate a realistic case. The test conditions refer to a nominal leak path length of 4.5 cm, crack heights of 0.25 and 1 mm, and a pressure difference of 4 Pa. The authors measured the particle penetration fraction for particle sizes 0.02–7 μm. Figure 3 shows the penetration fraction of particles for two different crack heights as calculated with our numerical model and compares the calculated results with the measured data. The flow was laminar, so only two deposition mechanisms are accounted for in the calculations in this work: namely Brownian diffusion and gravitational settling. The calculated results from the global model of Gelain (2007) are also shown. The following observations are made:

- As seen in Fig. 2, the model created for this work provides satisfactory results as compared with the measured data of Liu and Nazaroff.
- Generally, both models display similar performances, but the penetration fraction as calculated with Gelain's model (2007) underpredicts when the crack height is 1 mm and overpredicts when the crack height is 0.25 mm.
- Gelain's model (2007) goes abruptly to zero for large particles in the 0.25 mm case. The model developed for the current effort predicts that the penetration fraction will asymptotically reach zero, a behavior which is more consistent with the measured data.
- Overall, it is observed that particles with $d_p$<0.01 μm or $d_p$>4 μm will not penetrate a crack with a height less than 250 μm. This is in agreement with the results from Gelain and Vendel (2007).

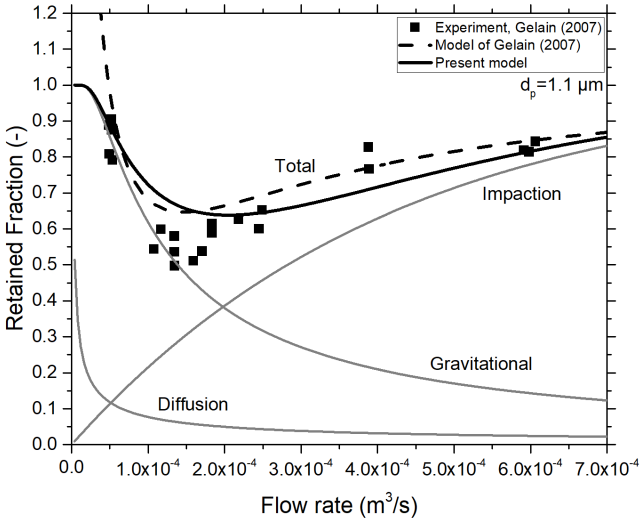


Fig. 1. Deposition fractions for particles of aerodynamic diameter of 1.1 μm.

## IV. RESULTS AND DISCUSSION

Particle penetration through CISCC was estimated by using the validated numerical model and considering the effects of three major deposition mechanisms: diffusion, gravitational settling, and inertial impaction. Particles are assumed to be spherical with a density of 8 g/cm$^3$ and with diameters ranging from 0.001 to 10 μm. The particle density was selected to represent particles with similar densities that may be released within a canister, such as $^{60}$Co from CRUD or $UO_2$ particles from fuel pellets. A uniform crack geometry is assumed throughout the channel, as well as a smooth inner surface and steady airflow through the crack. Three crack heights (crack opening) were selected: e=30 μm, e=50μm, and e=100 μm. Crack width was 10 mm, and crack length was 1.27 cm (0.5 in.). These dimensions are representative of real CISCC. In this case, the width of the crack in the third dimension is much larger than the crack opening so that airflow can be reasonably modeled as two dimensional without loss of generality. It is noted that in real cracks, irregular geometry and surface roughness might increase particle deposition significantly. This issue would be best explored by laboratory-scale experimental studies.

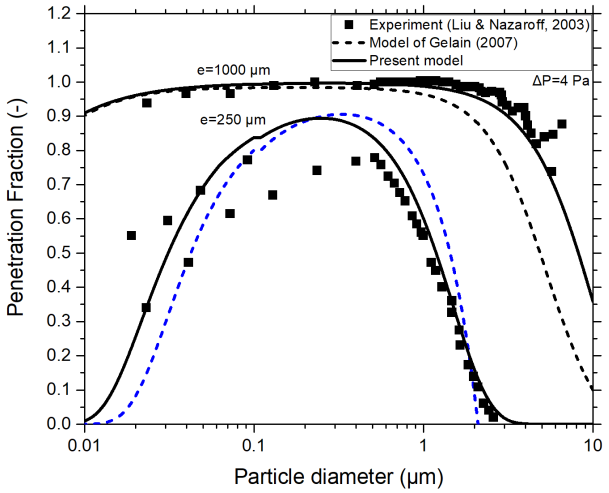


Fig. 2. Penetration fraction of particles as a function of particle diameter.

Fig. 3 shows particle penetration fractions for a crack height of 30 μm and three pressure differences: ΔP=50 Pa, 100 Pa, and 200 Pa. These higher-pressure differences were selected to better understand the required pressure that will allow significant particle penetration from such a small microcrack. The following observations can be made:

- The results suggest that particles having diameters in the range 0.1–0.5 μm have the highest penetration across the whole particle spectrum. This is in agreement with earlier results. Larger and smaller particles are readily removed in cracks under the gravitation settling and diffusion, respectively.
- The penetration factor becomes negligible for particles with diameters larger than 1 μm, even when a crack opening is 100 μm.
- For a crack height of 50 μm, particle penetration fraction is less than 30%. At a crack height of 100 μm, penetration is less than 90%. This translates to a reduction factor of 3, although crack height decreased by a factor of 2.
- For crack heights less than 30 μm, penetration is practically zero. This indicates that penetration varies strongly with crack height, and it significantly reduces with smaller crack heights.
- Figure 4 shows that a significant pressure difference, larger than 50 Pa, is needed for considerable penetration to occur from a 30 μm crack. Even when ΔP=200 Pa, penetration is less than 60%. For ΔP=50 Pa, penetration is less than 20%, and it is practically zero for smaller pressure difference.
- Fig. 4 shows regimes for aerosol transport through CISCC as a function of pressure difference. Practically no aerosol release is predicted for cracks with opening displacements or heights less than 50 μm when ambient conditions prevail. Furthermore, no particles with diameters >1 μm will be released for cracks with opening displacements or heights less than 100 μm.

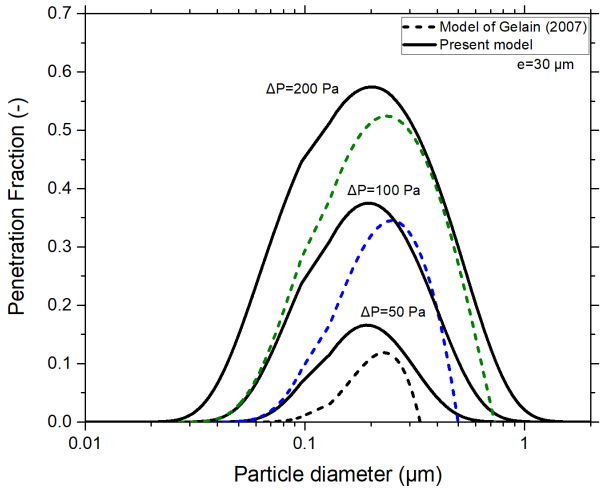


Fig. 3. Penetration fraction as a function of particle diameter for crack heights e=30 μm and ΔP=50 Pa, 100Pa, and 200 Pa.

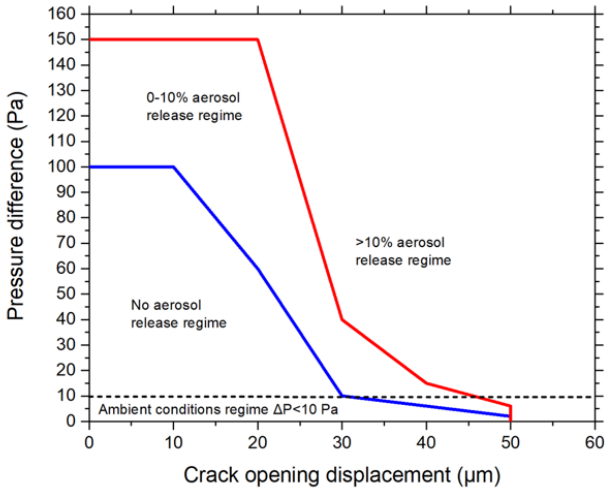


Fig. 4. Regimes for aerosol transport through CISCC as a function of pressure difference (penetration as a function of particle size spectrum is shown in upper right of figure). The term *ambient conditions* refers to conditions following canister depressurization. Highest penetration efficiency is observed for particles in the range of 0.1–0.5 μm. No particles with diameters >1 μm are expected to be released for cracks with opening displacement (height) less than 100 μm.

## V. SUMMARY

A numerical model was developed that enables the calculation of aerosol transport and retention in leak paths and that takes plugging formation into account. The model assumes a one-dimensional flow through a hydraulically

equivalent leak path. The description is dynamical (changing duct geometry due to plugging) and mechanistic. The Eulerian approach relies on the numerical solution of the aerosol transport equation in one dimension using finite differences. An extensive validation exercise was conducted based on comparisons with experimental measurements and empirical correlations. The model is fairly general since it is based on a generic mechanistic description of the aerosol flow and particle deposition in the leak path, without requiring experimental fittings other than using the leak rate parameters commonly available in practical applications. The model predictions are in approximate agreement with experimental data and reasonably representative.

The modeling calculations presented in this paper can provide important insight into the expected values of aerosol release through CISCC and the factors that affect it. However, particle penetration through cracks is sensitive to the minimum crack dimension. The lack of detailed information on the distribution of crack sizes limits the ability to extend the modeling results to real cracks. Nevertheless, information on the overall characteristics can be used to constrain the domain of practical interest. Further progress will require improvements to refine the model, in combination with experimental studies. Advances in this area hold the promise of improving the accuracy of consequence assessments by taking the leak path deposition of aerosol into account in the source term.

## ACKNOWLEDGMENTS

This material is based upon work supported by the US Department of Energy, Office of Nuclear Energy, under contract number DE-AC05-00OR22725.

## REFERENCES

1. EPRI, "Dry Cask Storage Welded Stainless Steel Canister Breach Consequence Analysis Scoping Study," Report no. 3002008192, Palo Alto, CA: EPRI (2017).

2. B. D. BOWEN, S. LEVINE, and N. EPSTEIN, "Fine Particle Deposition in Laminar Flow through Parallel Plate and Cylindrical Channels," *J. Colloids Interface Sci.* **54**, 375–390 (1976).

3. D. LIU and W. W. NAZAROFF, "Modeling Pollutant Penetration across Building Envelopes," *Atmos. Environ.* **35**, 4451–4462 (2001).

4. C. F. CLEMENT, "Aerosol Penetration through Capillaries and Leaks: Theory," *J. Aerosol Sci.* **26**, 369–385 (1995).

5. S. DURBIN, "Measurement of Particulate Retention in Microchannel Flows," Prepared for DOE, Spent Fuel and Waste Science and Technology Program, Sandia National Laboratories. Report no. SAND2018-10522 R, Revision 0 (2018).

6. R. B. MOSLEY et al., "Penetration of Ambient Fine Particles into the Indoor Environment," *Aerosol Sci. Technol.,* **34**, 127–136 (2001).

7. D. LIU and W. W. NAZAROFF, "Particle Penetration through Building Cracks," *Aerosol Sci. Technol.,* **37**, 565–573 (2003).

8. M. M. R. WILLIAMS, "Particle Deposition and Plugging in Tubes and Cracks (with Special Reference to Fission Product Retention)," *Progress in Nuclear Energy*. **28**, 1–60, (1994).

9. T. GELAIN and J. VENDEL, "Research Works on Contamination Transfers through Cracked Concrete Walls," *Nucl. Eng. Des.* **238**, 1159–1165 (2007).

10. Y. DROSSINOS and C. HOUSIADAS, *Aerosol Flows. In: Crowe, C. (Ed.)*, The Multiphase Flow Handbook, CRC Press – Taylor & Francis (Chapter 20) (2017).

11. C. N. FUCHS, *The Mechanics of Aerosols. Pergamon Press*, Oxford (1964).

12. R. K. SHAH and A. L. LONDON, *Laminar Flow Forced Convection in Ducts*, Academic Press (1978).

13. A. C. WELLS and A. C. CHAMBERLAIN, "Transport of Small Particles to Vertical Surfaces," *Brit. J. Appl. Phys.*, **18**, 1793–1799 (1967).

14. D. A. V. MORTON and J. P. MITCHELL, "Aerosol Penetration through Capillaries and Leaks Experimental Studies on the Influence of Pressure," *J. Aerosol Sci.*, **26**, 353–367 (1994).

15. D. MITRAKOS et al., "*A Simple Mechanistic Model for Particle Penetration and Plugging in Tubes and Cracks*," *Nucl. Eng. Des.*, **238**, 3370–3378 (2008).